

Flexural Behavior of Sustainable SCC Beams with Treated Recycled Aggregate and Steel Fibers: An Experimental and DIC Study

Abdullah Hamid Radhi Al-Rekabi

College of Science, University of Al-Qadisiyah, Ad Diwaniyah, Iraq.

E-mail: abdullah.hamid@qu.edu.iq

Received: 20 May 2025 | Revised: 23 July 2025 | Accepted: 25 August 2025 | Published: 04 September 2025

Abstract

This paper presents the findings of an experimental investigation into the performance of reinforced self-compacting concrete beams made of 100% recycled aggregates (RA). Three distinct types of steel fibers (SF) were utilized in the study: micro, hook-ended, and a hybrid of both, at varying percentages of 0.5% and 1%. A straightforward and economical treatment has been put forth, entailing the impregnation of recycled aggregates (RAs) with a cement-silica fume slurry (CSFS), with the objective of enhancing their characteristics. The experimental program comprised seven RA-SCC beams, which were divided into two distinct groups. The first group consists of two non-fibrous beams made with natural and recycled aggregate, while the second group includes five fibrous beams reinforced with steel fibers by two percentages, 0.5 and 1%, respectively. Furthermore, this study employed the DIC method to capture the deflection response, crack width, and crack pattern and morphology of the fibrous and non-fibrous beams with treated recycled aggregate, micro-SF, hooked SF, hybrid SF, and volume fraction of SF. The experimental findings indicated that the utilization of RA reduced the flexural strength of reinforcement SCC beams by approximately 12% in comparison to the reference beam. Notwithstanding the type and amount of fibers utilized, the incorporation of steel fibers yielded flexural performance that was commensurate with or exceeded that of the control beams. Furthermore, a comparison of the DIC data with the experimental results demonstrated the superior accuracy of the DIC method in comparison with visual inspection, particularly in the assessment of cracking loads.

Keywords: Sustainable, SCC, Reinforced Concrete, Structural Behaviour, Treated Recycled Aggregate, Hybrid Steel Fibres, DIC.

* Correspondence Author

Copyright: © 2025 by the authors. Licensee Scientific Steps International Publishing Services, Dubai, UAE. This article is an open access article distributed under the terms and conditions of the Creative Commons Attribution (CC BY) license (<https://creativecommons.org/licenses/by/4.0/>).

Cite This Article: Al-Rekabi, A. H. R. (2025). Flexural Behavior of Sustainable SCC Beams with Treated Recycled Aggregate and Steel Fibers: An Experimental and DIC Study. *Steps For Civil, Constructions and Environmental Engineering*, 3(3), 14-33. <https://doi.org/10.61706/sccee12011209>

Introduction

Reinforced Concrete (RC) is frequently utilized as the primary structural element in building construction. Concrete has historically been a highly sought-after construction material, and its importance is projected to persist into the future. Concrete is composed of a substantial amount of non-renewable mineral content and resources, particularly natural aggregate. Aggregates play a pivotal role in the composition of concrete and asphalt mixtures. In the conventional concrete mixture, the aggregate component constitutes 60% to 75% of the total volume. According to the findings of Behnood et al. (2015) and Hamad & Dawi (2017), global annual cement production was predicted at 4.7 billion tonnes in 2016 and 5 billion tonnes in 2020, with expectations indicating growth to 8 billion tonnes by 2027. Cement is predominantly employed in the production of concrete. It is estimated that the global production of concrete will exceed 25 billion tons per annum. The escalating consumption of natural aggregate resources, coupled with the diminution of high-quality aggregates, has precipitated a paucity of superior aggregates and engendered augmented costs due to the transportation of materials from distant areas.

The incorporation of recycled coarse aggregate (RCA) in construction projects has been demonstrated to contribute to the mitigation of environmental concerns and the conservation of non-renewable natural resources. The substitution of natural aggregates (NA) with recycled aggregates (RA) derived from crushed waste has become increasingly prevalent, as coarse particles play a substantial role in the concrete matrix's structure. The recycling of concrete from demolished structures presents a number of advantages. The implementation of this strategy has been demonstrated to result in a number of notable benefits, including but not limited to:

- The reduction of collection and utilization for renewable resources, such as natural aggregate.
- The decrease of landfill space.
- The enhancement of environmental quality by reducing air and groundwater pollution.

The conservation of millions of dollars within the construction sector (Alqarni et al., 2021). A substantial body of research has emerged in recent years, exploring the impact of incorporating recycled concrete aggregate in concrete manufacturing (André et al., 2014; Bravo et al., 2015; Panda & Bal, 2013; Pedro et al., 2015; Seo & Choi, 2014; Singh et al., 2020; Visintin et al., 2020; Yildirim et al., 2015).

The findings of this study indicate that the performance of recycled aggregate is often found to be inferior to that of conventional aggregate. This inferiority can be attributed to the presence of residual

cement particles, surface cracks, and higher water absorption and porosity in recycled concrete aggregate (RCA). The inaugural research on recycled aggregate in Japan was published in 1988 (Mukai & Kikuchi, 2023). The impact of RA on the concrete compressive strength has been examined in numerous studies (Chen et al., 2006; Jiang et al., 2014; S. C. Kou & Poon, 2009; Muhsin Farhood et al., 2018; Xia et al., 2021). In this context, Çakır (2014) assessed the effect of utilizing a full replacement ratio of recycled concrete aggregates (RCA) on the concrete's compressive strength (fcu). Research has demonstrated that the strength of concrete decreases by approximately 24% when a complete substitution of recycled concrete aggregate (RCA) is employed in lieu of concrete made with natural aggregate (NA). G. Bai et al. (2020) and Sayhood et al. (2019) observed a reduction in both compressive strength and splitting tensile strength in mixtures including recycled aggregates (RA). A substantial decline in the strength of concrete was observed when conventional aggregates were substituted with recycled materials (S.-C. Kou et al., 2012). Furthermore, Corinaldesi (2010) assessed the mechanical characteristics of concrete produced using recycled concrete aggregate. The achievement of the optimal concrete compressive strength can be accomplished through the incorporation of up to thirty percent recycled concrete aggregate (RCA). Sayhood et al. (2019) demonstrated that the utilization of 100% recycled aggregate (RA) led to a significant decrease of approximately 25% in compressive concrete strength and 20% in indirect splitting concrete strength. However, the characteristics of concrete based on RCA were found to be contingent upon the source of the utilized RCA (Çakır, 2014; S.-C. Kou et al., 2012). A substantial decline in concrete strength was observed with an escalation in the proportion of RA substitute. The substitution of normal aggregate with recycled aggregate resulted in a decline in tensile concrete strength of approximately 30% compared to NA concrete mixture. The extant literature on the subject primarily focuses on the properties of conventional concrete (CC); however, there is a paucity of research investigating the addition of recycled aggregate in self-compacting concrete (SCC) mixtures. Grdić et al. (2021) observed that self-compacting concrete (SCC) mixtures can be effectively produced from recycled aggregate (RA) at substitute ratios of 50% and 100%. However, an increase in the water content of the mixture was necessary to achieve the same slump flow spread when using a full substitution of recycled material. Consequently, this led to a detrimental impact on the mechanical properties of the prepared SCC mixes. RA exhibits a modest reduction in adhesion capacity within the interfacial transition zone (ITZ) when compared with NA (Wang et al., 2019). The interfacial transition zone (ITZ) is predominantly

influenced by the nature of the coarse aggregate employed and the water movement during the mortar paste-aggregate interaction in the hydration process (V. W. Y. Tam et al., 2018; Yehia et al., 2014; Yehia, Farrag, et al., 2015; Yehia, Helal, et al., 2015). Consequently, inadequate adhesion efficiency, in conjunction with the augmented interfacial transition zones, has a deleterious effect on the mechanical characteristics of recycled concrete aggregate (Wang et al., 2019; Yehia, Helal, et al., 2015). In consideration of structural performance, it was ascertained that the incorporation of recycled aggregate (RA) in reinforced-concrete constructions yielded a diminution in flexural strength, an augmentation in crack width, and an escalation in deflection values. Bai & Sun (2010) investigated the flexural behavior of reinforced concrete beams samples using various RA percentages and observed that the reduction in ultimate flexural capacity was mostly influenced by the RA replacement ratio. Additionally, it was observed that RA beams exhibited a greater propensity for cracking in comparison to the reference beams, which were designated as NA. Comparable results were additionally observed in the studies of Knaack and Kurama (2015) and Yang and Lee (2017). Arezoumandi et al. (2015) evaluated eight full-scale reinforced concrete beams with 100% recycled aggregate replacement and observed similar ultimate flexural strength, with a 13% increase in beam deflections. Seara-Paz et al. (2018) conducted a study on reinforced concrete beams that incorporated recycled aggregate in varying proportions. It was observed that an augmentation in the percentage of RA concrete resulted in a substantial diminution in the cracking moment. This phenomenon led to a more expeditious and perceptible cracking process in comparison to that of NA concrete. W.-C. Choi et al. (2012) advanced the hypothesis that recycled aggregate (RA) could be utilized as a suitable construction material in reinforced concrete, exhibiting a flexural performance that is analogous to that of natural aggregate (NA) beams. A comprehensive analysis revealed a substantial decrease of approximately 25% in the cracking moment, while the deflection remained consistent in RA self-compacting concrete beams when compared to the analogous reference beam. In a subsequent investigation by Ignjatović et al. (2013), nine full-scale beams with 50% and 100% recycled aggregate (RA) were utilized, and the deflection and flexural strength of RA beams were found to be equivalent to those of natural aggregate (NA) beams. Pradhan et al. (2018) indicated that RA beams exhibited an increased number of cracks, increased cracking propagation, and decreased flexural strength, indicating the inferior characteristics of RA. This phenomenon could be attributed to the progressive effect caused by remaining mortar particles in RA, microcracking, and its higher water absorption and porosity (Alqarni et al., 2021).

In order to resolve the aforementioned issue, a series of investigations were conducted, leading to the enhancement of RCA's efficiency through the implementation of treatment techniques (Shi et al., 2016; V. W. Y. Tam et al., 2007; V. W. Y. Tam & Tam, 2008; V. W.-Y.). As stated by Tam et al. (2006). The treatment procedures for RCA generally entail one of two approaches: either enhancing the adhering mortar or removing it. The enhancement of adhered mortar can be achieved through various methodologies, including the modification of concrete mixture ratios, the incorporation of cementitious components (SCM), the utilization of cementitious solutions, the carbonation process, the immersion of lime with carbonation, the coverage of recycled concrete aggregate (RCA) with organic or inorganic compounds, and the saturation of polyvinyl alcohol (PVA). One of the most economical, effective, and eco-friendly methods for improving the mechanical properties and durability of recycled concrete aggregates (RCA) is pre-soaking adhered cement mortar. A plethora of investigations have been conducted on the subject (Babu et al., 2014; Choi et al., 2016; State of the Aggregate Resource in Ontario Study). As demonstrated in the Consolidated Report (2010), enhancing the concrete mixing process resulted in an improvement in its compressive strength. Furthermore, researchers propose that incorporating silica fume and fly ash into recycled concrete aggregate (RCA) is the most effective method for improving compressive strength in concrete. A viable approach to mitigate the adverse effects of these treatments entails the preservation of the aged cement adhering to the recycled aggregates. This objective can be achieved by implementing an advanced treatment method for RA (Al-Rekabi et al., 2023; Al-Rekabi & Abo Dhaheer, 2024; Al-Rekabi & Daheer, 2024). These processes included the immersion of recycled aggregate pieces in a cement-silica fume slurry (CSFS) liquid prior to their incorporation into concrete mixtures. A substantial body of research has demonstrated that the incorporation of CSFS into RA concrete leads to enhanced mechanical characteristics (Al-Rekabi & Abo Dhaheer, 2024). Al-Rekabi & Abo Dhaheer (2024) conducted laboratory experiments to enhance the mechanical characteristics of RA-SCC mixes. The proposed treatment method has demonstrated effectiveness, as evidenced by the physical properties of treated RA, which exhibited increased specific gravity and reduced water absorption in comparison to untreated RA. In the case of untreated RA mixtures, the replacement of NA with RA resulted in a substantial decline in f_{cu} and f_{st} values. However, a marginal decrease in these values was observed when treated recycled aggregate was utilized in lieu of NA. Notwithstanding, this technique has inherent limitations and has not yielded a satisfactory resolution for the RA's physical imperfections.

A contemporary strategy to enhance the resilience of concrete is the integration of fibers. The utilization of steel fiber-reinforced concrete (SFRC) in columns and beams, where bending stresses are paramount, entails the partial substitution of steel fibers for stirrups, thereby enhancing the shear reinforcement capacity. A wide array of fiber forms is present, including steel fibers, synthetic fibers, glass fibers, and both natural organic and inorganic fibers. However, steel fibers are the most prevalent in the building. The effectiveness of steel fibers is determined by three different characteristics: The length-to-width ratio (L/d) of the steel fiber, the geometry of the steel fiber (straight or hook-ended) and its surface curvature, and the surface treatment used are the three factors to be considered. Surface deformation is frequently implemented to enhance adhesion between the matrix and the fiber. The utilized steel fibers possess a circular cross-section with diameters ranging from 0.2 millimeters to 1 millimeter, lengths varying from 10 millimeters to 60 millimeters, and an aspect ratio of less than 100. In order to enhance the binding between steel fibers and the concrete matrix, it is possible to alter the steel fibers through surface and mechanical modifications. The utilization of straight and hooked-end steel fibers in building applications has been extensively documented (Xie et al., 2021). The research indicates that the addition of SF in RA concrete has several advantages, such as improving tensile strength, bridging cracks, and distributing stresses within the RA concrete matrix (Ahmed & Lim, 2021). In a 2018 study, Mohammed Abd examined the impact of SF on the flexural behavior of reinforced SCC beams with RA. The primary factors examined in this study were the transverse reinforced ratio (stirrup spacing of 50 mm and 100 mm), RA, and steel fibers ($V_f = 0.5\%$). The resultant findings indicated that RA beams exhibited cracking moments that were 25% lower than those of NA beams. Furthermore, the cracking moments and maximum deflection of fibrous beams were found to exceed those of non-fibrous beams. The researchers further indicated that SF could be useful as a component of vertical reinforcement. Ghalehnovi et al. (2021) indicated that the incorporation of SF at a V_f of 2% led to a substantial enhancement in the cracking behavior and an improvement in the maximum load-bearing capacity of RA concrete beam samples. In comparison to non-fibrous beams constructed from self-consolidating concrete, fibrous reinforced concrete demonstrated larger cracking moments and maximum deflection (Ghalehnovi et al., 2021). Reinforced components composed of this concrete demonstrated improved shear performance with the incorporation of a certain volume percentage of steel fibers (Ghoneim et al., 2020; Kannam et al., 2018).

According to the extant literature, the majority of research studies employed manual or semi-digital methodologies to evaluate deflection, cracking patterns,

strain, and crack width of recycled reinforced self-compacting concrete members strengthened by steel fibers. These procedures are labor-intensive and susceptible to measurement errors, which can compromise the reliability of the results. Furthermore, acquiring measurements at or in close proximity to the point of failure is frequently arduous due to the inherent risks to technicians and equipment posed by the projectiles resulting from the failure of specimens. Digital Image Correlation (DIC) is a contemporary optical technique that is employed to measure deformation and strain throughout entire materials or structural components via feature tracking and image registration (Peters et al., 1983). The DIC approach integrates deformation theory with visual inspection, thereby generating digital images of the specimen both prior to and following deformation. Subsequent to this, the images are examined to ascertain the disparity in the displacement field, thereby illustrating the strain distribution on the deformed surfaces of the samples. A considerable body of research has been dedicated to the application of this methodology, which involves the integration of the DIC technique with micrographic imaging, for the purpose of investigating stresses at the microscale. Gencturk et al. (2014) conducted an investigation of a full-scale prestressed concrete structure and recorded the advantages and disadvantages of the DIC strategy. The researchers employed stereo 3D-DIC to assess strain and displacement in an integrated field when utilizing standard displacement transducers. The testing procedure involved subjecting the prestressed I-beam to strain until it reached the point of failure. The findings indicated that DIC facilitated highly precise and comprehensive measurements of movement and stress, which were not attainable through earlier counting methodologies. The application of Digital Image Correlation (DIC) for the evaluation of concrete beams has been shown to be fraught with difficulties. These include the impact of lighting, the loss of data when the surface is damaged after spalling, challenges in measuring surface preparations, and the inability of the DIC method to locate and measure the width of cracks (Gencturk et al., 2014). Alam et al. (2014, 2015) employed a combination of acoustic emission and digital image correlation (DIC) techniques to investigate concrete fracture mechanisms, examining factors such as the extent of the fracture zone, crack openings, and crack tip characteristics. In order to assess and describe the initiation and development of concrete cracks, Alam et al. (2014, 2015) studied concrete beams with geometric scales. The study indicates that the combination of the two methodologies offers an effective tool for measuring fractures and cracks in concrete. The DIC method was employed to assess the integrity of cracks in walls and beams that had undergone substantial reinforcement (Ruocci et al.,

2016). A post-processing technique was employed to mitigate noise in full-field DIC measurements. The validity of this methodology has been substantiated through the examination of both full-scale and one-third-scale reinforced concrete beams under four-point bending conditions. The efficacy of the noise filtering technique in the post-processing of DIC data has been demonstrated, yielding precise estimates of strain and displacement (Ruocci et al., 2016). Gali & Subramaniam (2017) employed Digital Image Correlation (DIC) to analyze shear cracks and full-field deformation with the objective of characterizing the shear strength of fiber-reinforced concrete beams. A substantial body of research has demonstrated that the DIC method facilitates the observation of material behavior subsequent to the formation of shear fractures. Suryanto et al. (2017) employed Digital Image Correlation (DIC) to identify shear cracks in reinforced concrete (RC) beams and to examine the impact of reinforcement spacing on ductility, strength, and failure modes. The employment of DIC full-field deformation maps has enhanced the clarity of the investigation into longitudinal strain fields and post-cracking responses, thereby facilitating the monitoring of crack progression. The flexural reaction of reinforced concrete (RC) beams subjected to monotonic four-point bending loads and strengthened by non-structural matrix (NSM) fiber-reinforced polymer (FRP) bars was examined by Daghash & Ozbulut (2017). The strain maps and deflection were captured using the digital image correlation (DIC) method, while the strain response was recorded using strain gauges. The mid-span detection was computed by the DIC using the constant area of every beam, allowing for the capture of the major strain and cracking distribution of the beam. A study conducted by Ghahremannejad et al. (2018) examined the cracking performance of concrete beams reinforced with synthetic fibers using the digital image correlation (DIC) method. The findings have demonstrated that the readings from both the gauge and the DIC were consistent, with a maximum discrepancy of 10%.

The present study investigates the viability of employing the DIC technique to comprehensively capture the process of crack formation, the load-deflection response, and the morphology of cracks in recycled reinforced concrete beams that have been strengthened by a range of steel fibers. This investigation is conducted with meticulous attention to detail, aiming to elucidate the potential applications and limitations of the DIC technique in this specific context. A substantial body of research has been dedicated to the structural performance of reinforced normal vibrated concrete (NVC) rather than self-compacting concrete (SCC). Therefore, a comparison is presented and evaluated between experimental and DIC load deflection curves for RC-SCC beams made with 100% RA strengthened in flexure by hybrid steel fibers.

Additionally, the cracking morphology was investigated by analyzing the correlations between different gray values of digital images. This analysis was used to assess the cracking behavior in all surfaces of the tested beams. Two varieties of SF, designated as hook-ended and straight short (micro), were utilized at two distinct volume fractions of 0.5% and 1%. A hybrid SF, incorporating both micro and hook components, with a volume fraction of 1%, was utilized. This study provides substantial insights into the initiation and propagation of cracks through a measurement system that utilizes image analysis, assisted by a digital recording camera. This system facilitates precise identification of the initial crack, calculates the crack opening, and monitors the progressive cracking process until failure.

Experimental Work

Materials Properties

In this study, Ordinary Portland cement (Type I) that met the Iraqi requirements was used (IQS 5, 1984). A fine gray powdered material, referred to as silica fume, was used in the formulation of a cement-silica fume slurry (CSFS slurry). This slurry was utilized for the treatment of recycled aggregate (soaking) before its incorporation in SCC mixtures. The silica fume utilized in this study adheres to the specifications outlined in ASTM C1240-04 (ASTM International, 2000). In the production of mixtures for SCC, the use of limestone powder (LP) was employed to prevent segregation, thereby ensuring optimal flowability and cohesion. All filler and binder materials met the European Guidelines for Self-Compacting Concrete (SCC) (EFNARC, 2005). The SCC concrete mix was formulated using recycled aggregate (RA) as a substitute for natural coarse aggregate in the prepared mixtures. The present study incorporated three distinct categories of aggregate: natural aggregate (NA), untreated recycled aggregate (Untreated RA), and treated recycled aggregate (TRA), utilized as coarse aggregate. The formation of RA is attributed to the compression of preexisting cubes, with slab specimens being present at the College of Engineering. The experiment incorporated locally sourced sand, with a maximum size of 4.75 millimeters, as the fine aggregate when utilized in conjunction with the coarse aggregate. It is evident that all coarse and fine aggregates align with the IQS (IQS 45, 1984). In this study, a highly efficient water-reducing chemical mixture, referred to as GLENIUM® 54, was utilized. The product under consideration meets the requirement of ASTM C-494 (ASTM International, 2019). To enhance the structural integrity of the SCC beams, steel bars with diameters of 10 mm and 16 mm were utilized to resist flexure. The yield strengths of these bars were found to be 552.0 MPa and 560.5 MPa, respectively, while their ultimate strengths were determined to be 667.9 MPa and 659.8 MPa.

These values exceed the minimum requirement of 420 MPa established by ASTM A615 (ASTM International, 2022) for Grade 60 steel. Consequently, the bars meet the stipulated standard specifications. Additionally, the bars exhibited a modulus of elasticity of 200×10^3 MPa. In the steel fibers strengthening system, two steel fibers were utilized: micro and hooked fibers. The diameter of the former was 0.2 mm, while the diameter of the latter was 0.5 mm. The steel fibers provided by the manufacturer had an ultimate tensile strength of 2850 MPa and 1300 MPa for micro and hooked SF, respectively. The length of MSF was 12 millimeters, and the length of HSF was 30 millimeters. Furthermore, the aspect ratio for all fibre types was found to be 60.

Mix Proportions

The mixture proportions were developed based on the rational and efficient mix proportioning methodology provided in Abo Dhaheer et al. (2016a, 2016b), considering the specific characteristics of RA and the targeted mechanical performance. A series of SCC mixes were formulated with water-to-cement ratios ranging from 0.44 to 0.50. In order to facilitate the proportioning of SCC mixes, charts were developed. These charts are applicable to a broad spectrum of water-to-cement ratios and include a compressive strength class that is designated as a design parameter. The final mix was selected based on the results of these trials and consisted of 400 kg/m³ of cement, 770 kg/m³ of sand, 130 kg/m³ of limestone powder, and 176 kg/m³ of water, with a water-to-cement ratio of 0.44. However, the amounts of coarse aggregate, superplasticizer, and steel fiber were documented in **Table 1** for the normal concrete mix, treated recycled concrete mix, 0.5% fibrous concrete mix, and 1% fibrous concrete mix.

Specimen Details and Fabrication

The experimental study encompassed seven SCC beam specimens, each with dimensions of 250 millimeters in depth, 150 millimeters in width, and 1700 millimeters in length. The beams were designed in accordance with ACI 318-19 (ACI Committee 318, 2019) and tested under two-point loads spaced at a distance of 450 millimeters, continuing until failure. As illustrated in Figure 1, the beams under consideration are characterized by specific details. The SCC beams were then categorized into three groups, as shown in **Table 1**, based on the strengthening plan by steel fibers. The initial group consists of two SCC beams devoid of steel fibers (non-fibrous beams) employing standard and treated recycled aggregate. Conversely, the second group consisted of two fibrous beams that were strengthened by micro-SF with 0.5 and 1% V_f using treated recycled aggregate, as illustrated in Table 1. However, the third group contained two fibrous beams (Hooked SF) with 0.5 and 1% V_f . Finally, the remaining beam contained a hybrid SF (micro hooked SF) composition with 1% V_f . The reinforcement details for all groups of beams included two Ø16 mm steel bars placed in the tensile zone and one Ø10 mm bar in the compression zone. The shear reinforcement comprised Ø10 mm closed-loop steel stirrups, with a spacing of 103 mm between each stirrup along the shear spans. A uniform concrete cover of 25 mm was maintained on all sides of the structure. For the purpose of conducting research, Ø10 mm stirrups were installed in proximity to the supports and beneath the two-point loads within each group (**Figure 1**). In the experimental design, one beam was designated as the control beam and was left with normal aggregate. The testing of all seven SCC beam specimens was conducted at the Structural Engineering Laboratory, College of Engineering, University of Al-Qadisiyah.

Table 1. Proportional Mixture of Normal and Recycled Concrete Mixes (Kg/m³).

Mix Designation	Superplasticizers (Kg/m ³)	Coarse Aggregate (Kg/m ³)	Steel Fiber Content (kg/m ³)	Fiber Type	Fiber Volume Fraction (%)
F-NA-Ref	4.4	840	0	--	0
F-RA-Ref	4.8	780	0	--	0
F-RA-0.5MS	5.3	767	39	Micro	0.5
F-RA-1MS	6.5	754	78	Micro	1.0
F-RA-0.5HS	5.3	767	39	Hooked	0.5
F-RA-1HS	6.5	754	78	Hooked	1.0
F-RA-HYS	6.5	754	78	Hybrid	0.5 Micro+ 0.5 Hooked

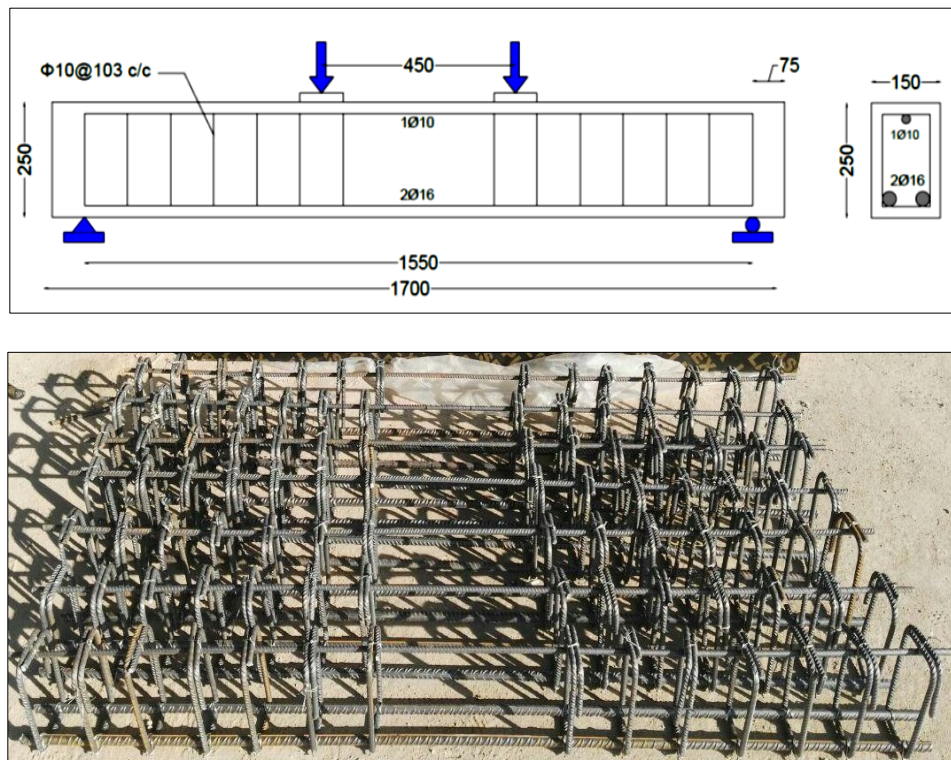


Figure 1. Geometric and Reinforcing Specifications of all Studied Beams.

Test Setup and Instrumentations

The tested beam has been designed in accordance with ACI 318-19 (ACI Committee 318, 2019). The beam samples were tested using a universal testing device with a maximum load capacity of 2000 kN (Figure 2). The instrumentation was accessible in the Structural Lab of the Civil Engineering Department at Al-Qadisiyah University. The test apparatus comprised a hydraulic actuator, a load cell, and a supporting system. The uniform distribution of imposed loads was achieved by utilizing steel plates. The beam specimens were kept in a dry state within the laboratory for a period of 28 days, after which they were painted white on their external surfaces. This method was employed to facilitate the monitoring of crack patterns during the test, as illustrated in Figure 3. A digital dial gauge, with a maximum rating of 50 millimeters, was employed to measure the deflection at the midpoint of the beam (the point of maximal flexural moment) in relation to the applied load. Subsequent to the beam's placement within the testing apparatus, it underwent horizontal adjustment at the test rig's center. Dial gauge devices were then meticulously positioned and affixed at their designated locations. The load was applied incrementally, with an initial increase of approximately 5 kN up to the first crack stage. Thereafter, the increment rate was increased to 10 kN until the ultimate load was reached. During the test, the load value of the first crack was used to indicate the crack propagation. The experiment was conducted until one of the cases reached a predetermined milestone. Firstly, a substantial decrease in the aggregate applied load values

is observed. Secondly, it was observed that deformations and crack widening occurred concurrently under identical loading conditions of the beam. Consequently, the concrete would undergo a process of fragmentation.

Digital Image Correlation

The general behavior of the tested beams was assessed and monitored by using an alternative or complementary methodology (known as digital image correlation, DIC, Figure 4). The research team employed a digital recording camera (Nikon) to record the study's audio component. The DIC technique was utilized to assess the beam's behavior in terms of load-deflection response and to investigate crack development, crack width, and crack spacing. The GOM correlate software package 2019 was utilized in this study, as illustrated in Figure 5. The DIC non-contact measuring technique was executed on one side of the beam. The utilization of the DIC-based tool was undertaken for the purpose of analyzing the material behavior exhibited by the specimens under conditions of applied loading. The system was configured to capture digital images and then employ 2D image correlation to assess deformation and strain. The calibration process, facilitated by a black-and-white grid, enabled a precise comparison between the undeformed and deformed states. Each image corresponded to a specific loading stage, with stage 0 representing the undeformed reference. The following steps were taken to apply this method: firstly, the beam side was coated with a layer of white paint, and a black

spot measuring approximately 2 mm was marked on the beam surface (**Figure 6**). Secondly, a camera must be installed in front of the black spots on the coated surface of the beam. The digital recording camera (Nikon D7200) employed for this purpose boasts a 23.5×15.6 mm sensor, with a resolution of 24.2 megapixels, as illustrated in **Figure 7**. This methodological approach facilitated a comprehensive evaluation of failure mechanisms, displacements, and strain distributions. It is imperative to maintain the camera's position during the testing process to ensure the integrity of the data

collected. Therefore, the camera was meticulously positioned in a location devoid of any nearby movement, airflow, or vibration that could potentially introduce disturbances or noise into the results. Thirdly, to achieve a more precise image, external light was directed toward the black-spots-coated surface of the beam. Finally, the results obtained by the DIC demonstrate a close relationship between the movement of black spots during the test and their initial condition. Therefore, it is imperative to take a reference image at the onset of the test.



Figure 2. Test Set Up Used in the Study.



Figure 3. Preparing the Beam Specimens.



Figure 4. The Digital Image Correlation Technique.

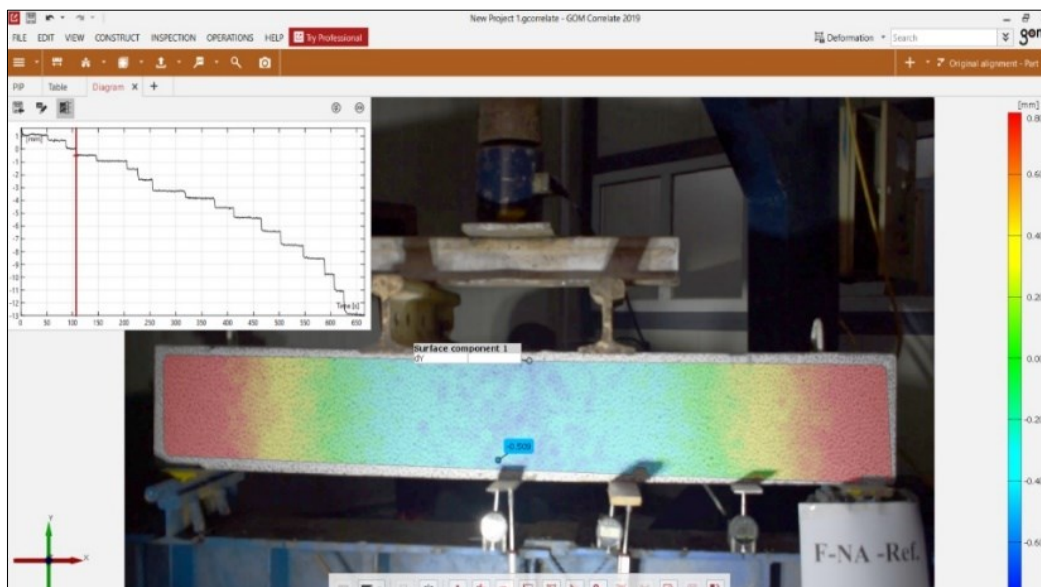


Figure 5. GOM Software Package 2019 Used in DIC.



Figure 6. Random Black Spots at the Beam Surface.



Figure 7. Nikon Camera Used for DIC Method.

GOM Correlate Software Package 2019

The program utilized in DIC technology was GOM Correlate software package 2019 (as illustrated in **Figure 8**). The software under consideration offers a cost-effective solution for any specimens that are tested by means of a digital camera. In this program, 2D digital image correlation was utilized to assist in the evaluation of a series of digital images. The imported images facilitate expeditious access to the aggregate result data sets. The GOM software package technique utilized the black and white grid distribution for the calibration of images and the comparison of the relative locations of deformed and un-deformed images. Each recording image corresponds to a distinct phase in the loading procedure. The initial image in GOM corresponds to stage 0 and is regarded as a reference image for the un-

deformed specimen. In this study, the failure mode, displacement, crack propagation, and crack width were measured using the GOM software package, which employs digital image correlation (DIC) technology.

Results

This section presents and discusses the experimental test results, as shown in **Table 2**, including the first crack load, failure load, and failure mode of the SCC beams made with treated recycled aggregate strengthened by a variety of steel fibers. Furthermore, the section presents a comparison of the displacements of the strengthened beams captured using the DIC method with those recorded experimentally by the dial gauge.

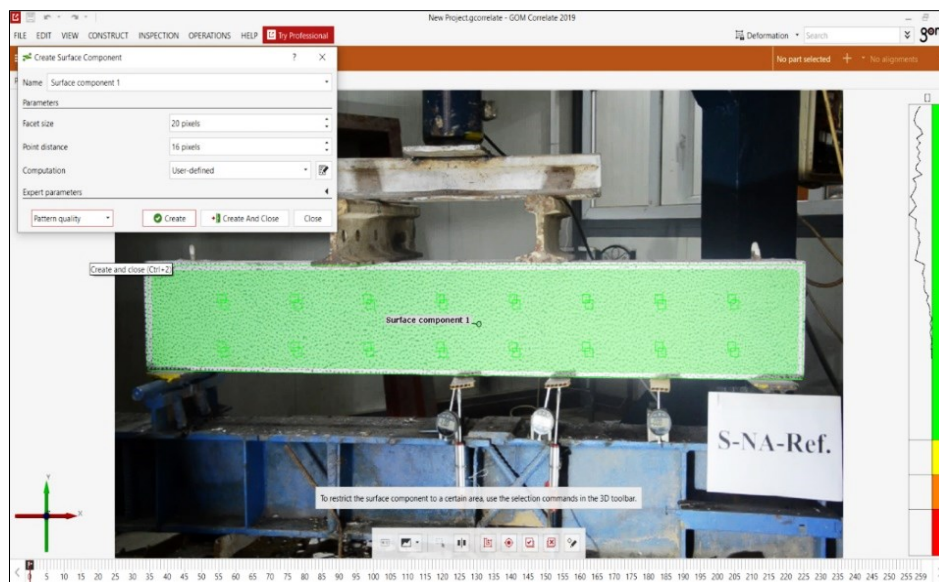


Figure 8. GOM Software Used in the DIC.

Table 2. Characteristics of Respondents

Beams Notation	First Crack Load (kN) (P_{crf})	Δ_{max} *	Failure Load P_u (kN)	Change in P_u %	Mode of Failure
F-NA-Ref	39	12.70	225	--	Flexural mode failure
F-RA-Ref	32	12.30	199	- 11.56	Flexural mode failure
F-RA-0.5M	40	13.10	249	+10.67	Flexural mode failure
F-RA-1M	57	12.80	265	+17.78	Flexural mode failure
F-RA-0.5H	42	13.80	245	+8.89	Flexural mode failure
F-RA-1H	65	13.30	255	+13.33	Flexural mode failure
F-RA-HYS	73	14.97	269	+19.56	Flexural mode failure

Δ_{max} = Maximum mid-span deflection (mm)

Load-Deflection Response

The mid-span vertical deflection of a beam can be readily calculated by employing the GOM program in

the DIC technique at any point on the specimen's surface. Monitoring of the system can be conducted at any point during load testing in the displacement field or during load testing in the laboratory. In this study, the

validity of the DIC methodology was validated by comparing its load-deflection results with those obtained from the experimental dial gauge at the point near the bottom edge of the specimen mid-span (close to the dial gauge point, as shown in **Figure 9**). As illustrated in **Figure 10**, the dial gauge load-deflection curve is presented in conjunction with the DIC load-deflection curve. It was observed that the RA beam exhibited a lower degree of stiffness compared to the NA-Ref beam, which was composed exclusively of natural aggregate. These findings were in agreement with those reported in (Al-Rekabi et al., 2023; Al-Rekabi & Abo Dhaheer, 2024; Al-Rekabi & Daheer, 2024). The weak interfacial transition zones (ITZs) that affect the bond between RA surfaces and cement mortar may be the reason for the reduced flexural capacity of the RA-Ref beam.

As demonstrated in **Table 2** and **Figure 10**, the efficacy of the steel fibers utilized in enhancing the stiffness of reinforced concrete (RC) beams, denoted as P_u , is evident. The fibrous RA beams demonstrated higher stiffness compared to the non-fibrous beams, particularly when V_f of 1% was incorporated. Furthermore, the respective increases in ultimate load for the F-RA-0.5M, F-RA-1M, F-RA-0.5H, F-RA-1H, and F-RA-HY beams were 11%, 18%, 9%, 13%, and 20%, respectively, compared with NA beams. Meanwhile, the respective increases were 25%, 33%, 23%, 28%, and 35%, respectively, compared with RA beams. This phenomenon has also been observed in reinforced normal vibrated concrete (Ghalehnovi et al., 2021; Mohammed Abd, 2018). The test results indicate

that the incorporation of steel fibers, particularly at a volume fraction of 1%, can significantly enhance the cracking loads ($P_{(crf)}$) of reinforced concrete (RC) beams. These enhancements are found to be predominantly influenced by the volume fraction of steel fibers. It has been demonstrated that the $P_{(crf)}$ increases in proportion to the magnitude of the SF volume fraction. In consideration of the utilized SF, hybrid fiber-reinforced beams demonstrated the highest $P_{(crf)}$ compared to other fibrous beams. The respective increases in F-RA-1M and F-RA-1H beams were 46% and 67%, respectively, compared with 87% in the F-RA-HY beam. In this case, the integration of hybrid SF effectively addresses both micro- and macro-cracks present within the RA concrete matrix. The micro-SF has been demonstrated to arrest micro-cracks, while the hooked SF fibers have been shown to prevent or minimize the formation of macro-cracks. Consequently, this enhances both the flexural cracking and ultimate loads of RA beam, as well as its deformation capacity.

Conversely, the comparison suggests that both test results exhibited a certain degree of similarity. This agreement serves to substantiate the efficacy of the DIC method in predicting displacements at any given point along the beam. As illustrated in **Figure 10**, the discrepancy between the dial gauge and the DIC test results exhibited a high degree of concurrence in beams devoid of fibrous materials. However, a lesser degree of consensus was observed in fibrous beams. This discrepancy could be attributed to the concentration and distribution of fibers within the concrete matrix, particularly when 1% V_f was incorporated.

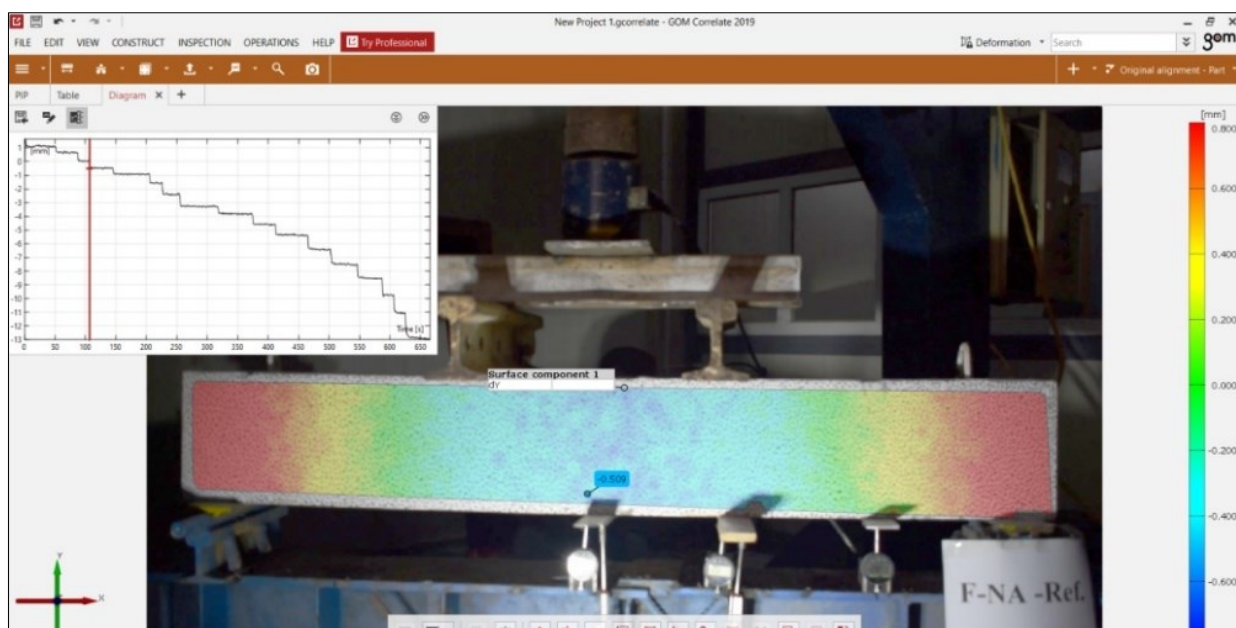
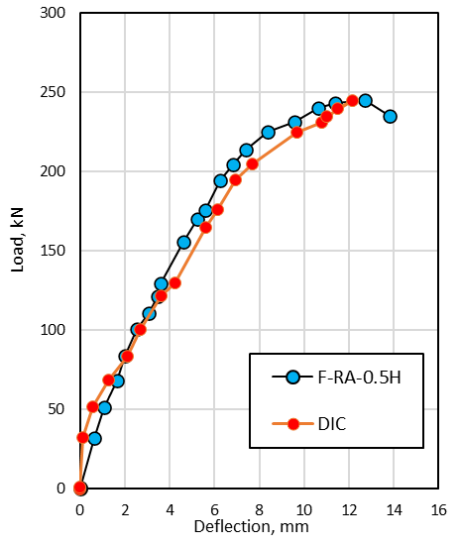
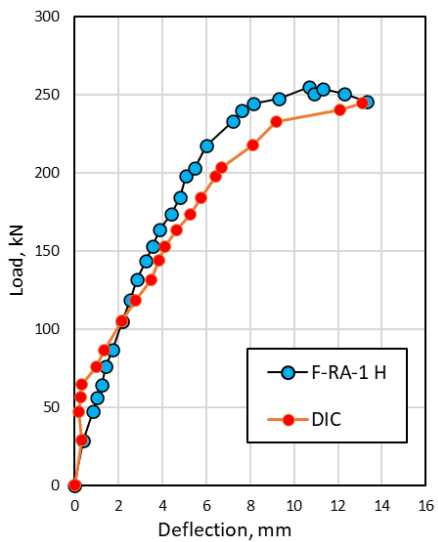
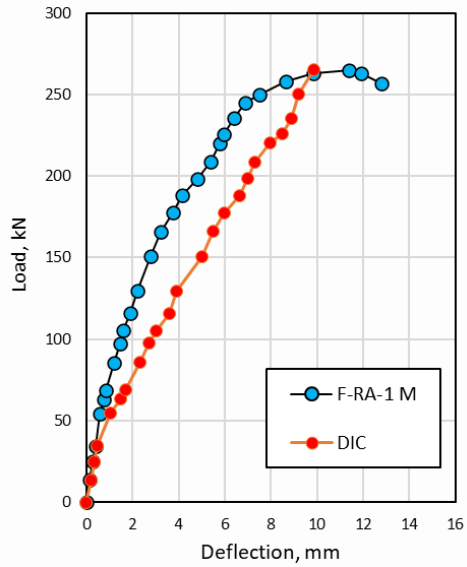
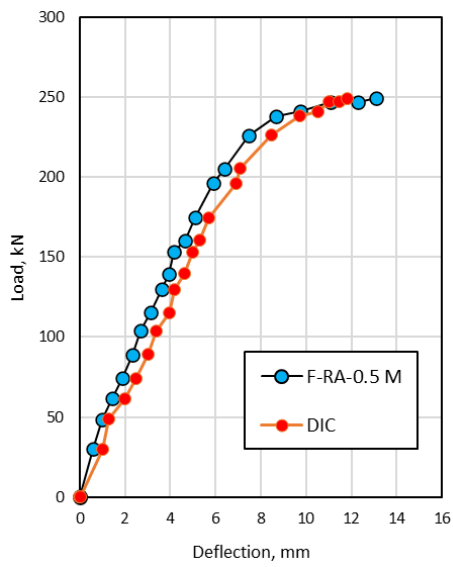
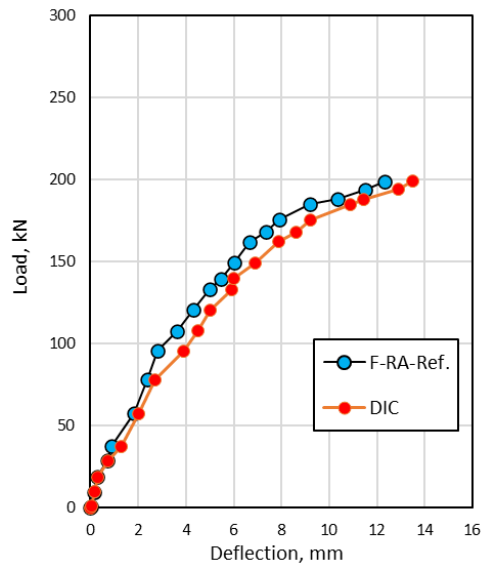
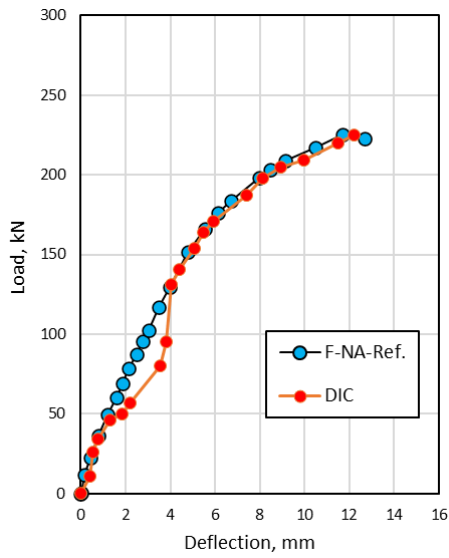


Figure 9. Representative Vertically Deflection of Test Beams Evaluated by Digital Image Correlation (F-NA-Ref).



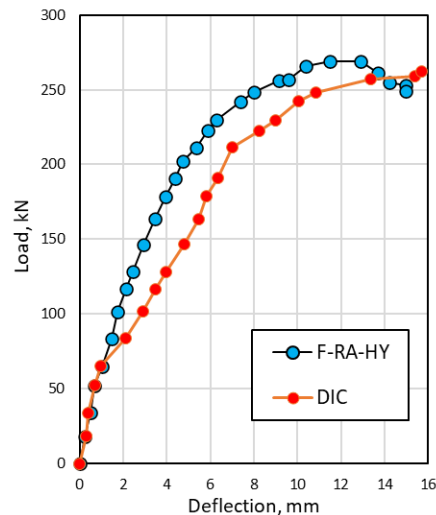


Figure 10. Load-Deflection Curve of Tested Beams Measured by Dial Gauge and DIC Technique.

Crack Patterns and Crack Development

This study employed the DIC method to analyze the cracking patterns and their progression throughout the testing process. The recorded pictures are then subjected to analysis at varying load levels in contrast to the reference images obtained prior to loading. The cracking pattern and developing crack during the load transfer are illustrated in **Figures 11–12**. The cracking patterns and distribution of the testing beams were meticulously documented through the use of the Digital Image Correlation (DIC) method. It is noteworthy that during the stage of crack formation, cracks developed at critical zones, typically vertical, originating from the mid-beam areas (the major positive moment area). The formation and propagation of diagonal cracks was observed to occur in conjunction with increasing bending moments. Subsequently, the preexisting fissures expanded, accompanied by the emergence of additional minor cracks. A comparison of the crack patterns of RA and NA beams revealed that they were generally identical. This assertion is corroborated by extant research (Arezoumandi et al., 2015; Kou & Poon, 2009). It was observed that the fibrous RA beams exhibited finer and more closely developed cracks compared with non-fibrous ones. This phenomenon may be attributed to the following hypothesis: SF facilitates stress redistribution due to its superior fiber bridging capability. In the vicinity of the crack, SF facilitates the transfer of high stresses to the surrounding concrete matrix, leading to the formation of additional vertical and diagonal cracks (Ghalehnovi et al., 2021).

Crack Width

In this study, crack width was determined using two methods: (1) a crack-meter, and (2) DIC technology. For each loading stage, the crack width was determined using GOM software's 2D digital picture correlation. As demonstrated in **Figure 13**, the width of the crack that

developed was measured from the initial crack at mid-span until the maximum width of the fibrous specimen. The width was measured at the maximum positive moment and load support regions at each step of the applied load. An optical micrometer was utilized for this purpose. As illustrated in **Figure 13**, the relationship between the crack width and the applied loads of the SCC beam specimens with SF is demonstrated. The incorporation of SF has been demonstrated to exert a favorable influence on the reduction of crack widths in RA-based beams, thereby constraining their propagation. In this concept, the beam crack width was predominantly influenced by the type of steel fibers and their volume fractions. However, the crack exhibited a greater tendency to be governed by the former parameter in comparison to the latter. Conversely, it was indicated that there was a substantial agreement between the crack widths obtained from the crack-meter and the Digital Image Correlation (DIC) technique. Consequently, the DIC technique can be used as an alternative to the crack meter to assess the width of cracks throughout the test. This approach can reduce testing time and provide values for the width of any formed propagated crack at any loading stage.

Conclusion

- The objective of this study was to ascertain the viability of leveraging Digital Image Correlation (DIC) technology to assess the load-displacement characteristics, crack pattern, and crack width of RA-SCC beam specimens with varying steel fibers. A comparative analysis was conducted between the DIC results and the experimental data, which yielded the following findings:
- The study's findings indicate that the incorporation of 100% untreated recycled aggregate (RA) in SCC beams results in a reduction of approximately 12% in flexural capacity. This decline can be attributed to the inherent weaknesses of RA, which are not fully

addressed by the use of RA. However, this deficiency can be effectively mitigated by the incorporation of steel fibers.

- Hybrid fiber-reinforced beams exhibited an augmented flexural cracking load, demonstrating an increase of approximately 87% in comparison to other fibrous beams. The respective increase was 46% and 67% when micro and hooked steel fibers were utilized.
- At a 1% fiber volume, the ultimate flexural load exhibited an 18%, 13%, and 20% increase for the RA-1M, RA-1H, and RA-HY beams, respectively, compared to the natural aggregate reference beam (F-NA-Ref).
- The DIC method employed in this investigation appears to be a suitable approach for assessing the deformation of reinforced SCC beams. This method effectively captures the load-deflection responses

during flexural failure modes, making it a valuable tool for analyzing structural behavior.

- The DIC technique has been employed to ascertain the crack width that develops within the test. This approach has the potential to reduce the time required for testing and to provide precise measurements of the width of any cracks that may be present in the tested members.
- The DIC method has been shown to identify and detect early crack formation, whereas the standard method cannot do so until the loading reaches a level that has already produced specimen cracking or rupture.
- DIC exhibited a marked superiority over conventional instruments by completely manifesting the cracking morphology in reinforced concrete specimens that were subjected to testing.

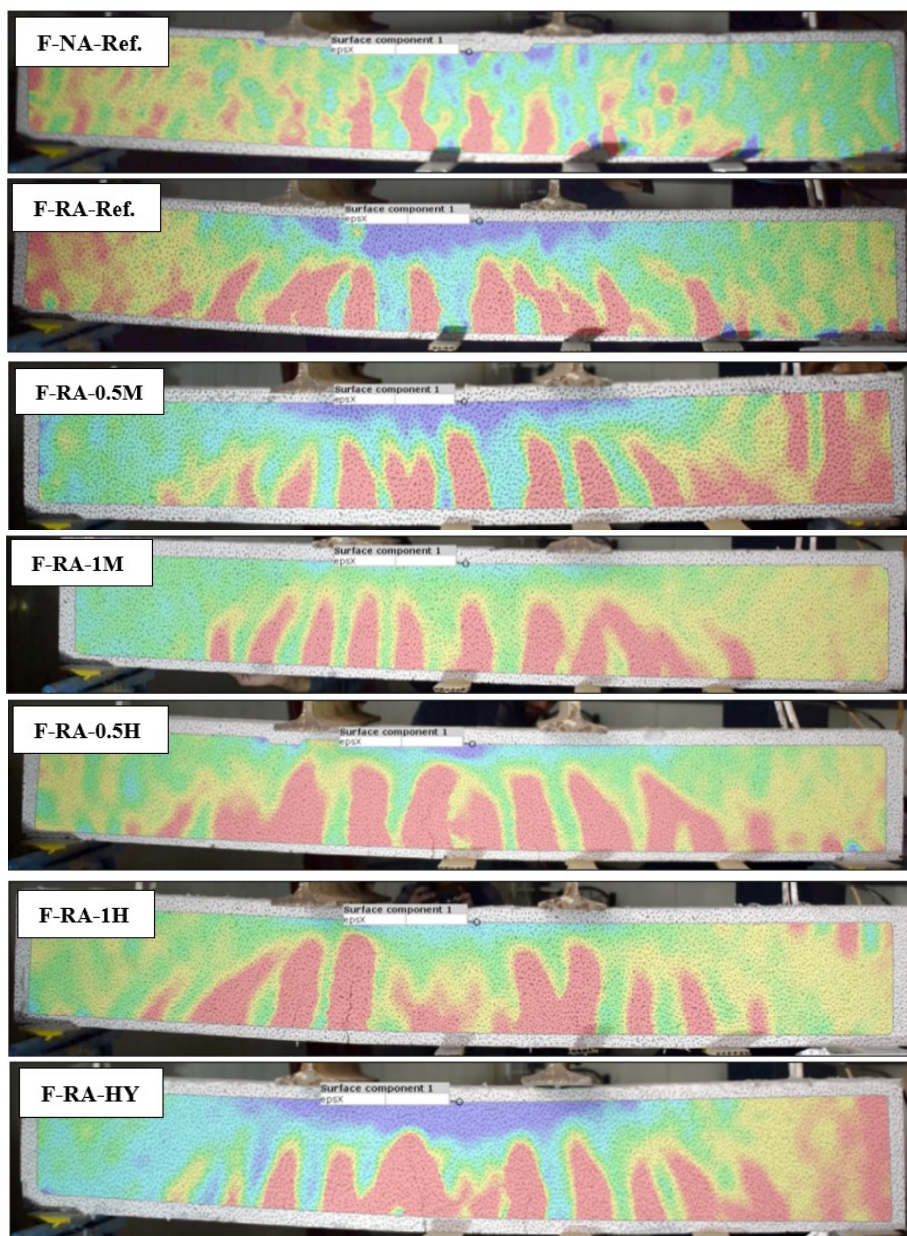


Figure 11. Crack Pattern of Tested Beams:

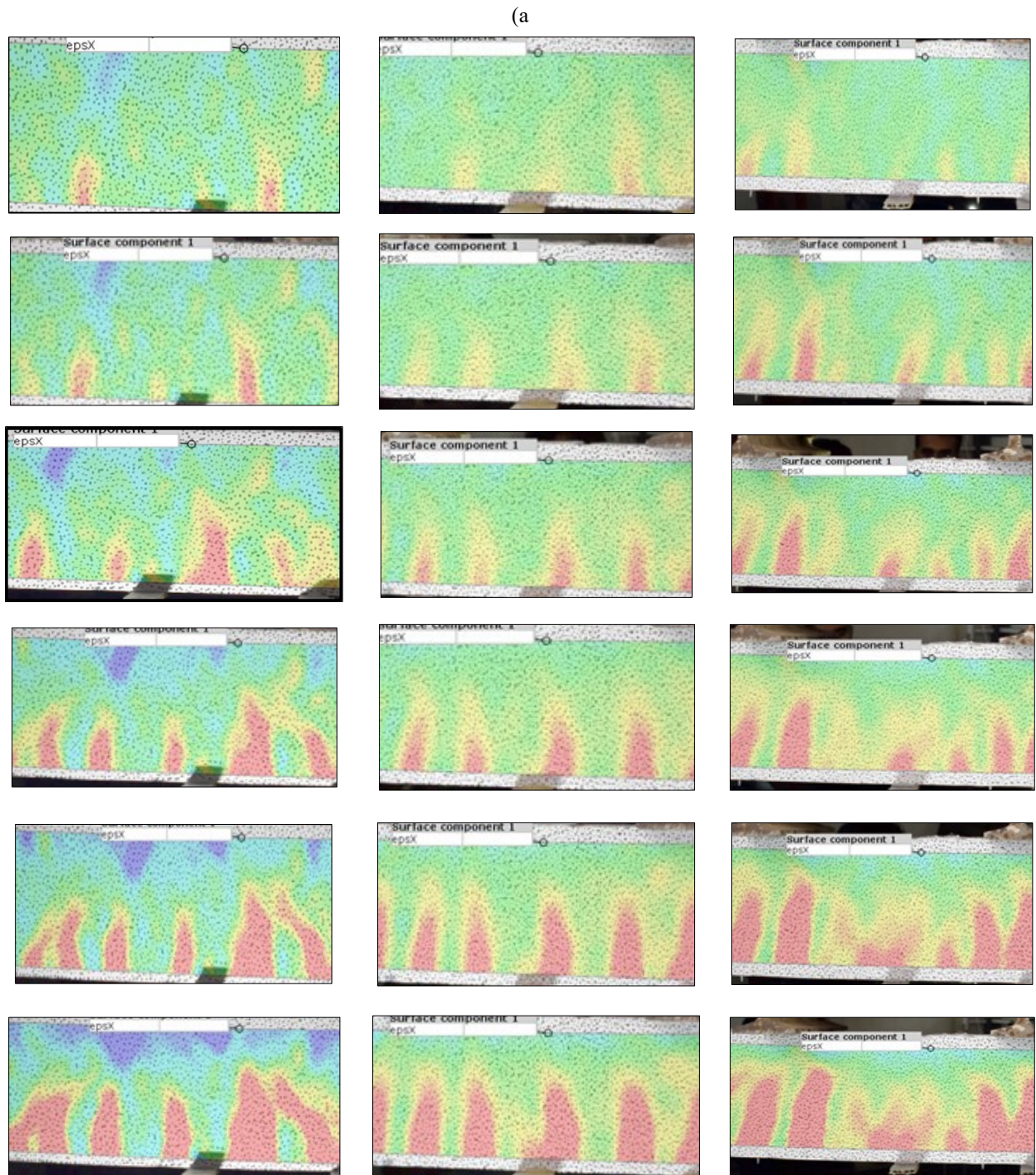


Figure 12. Cracks Development in the Corresponding Ultimate Load Stage of F-RA-Ref. (left), F-RA-1 M (Middle), and F-RA-1 H (Right) Beams.

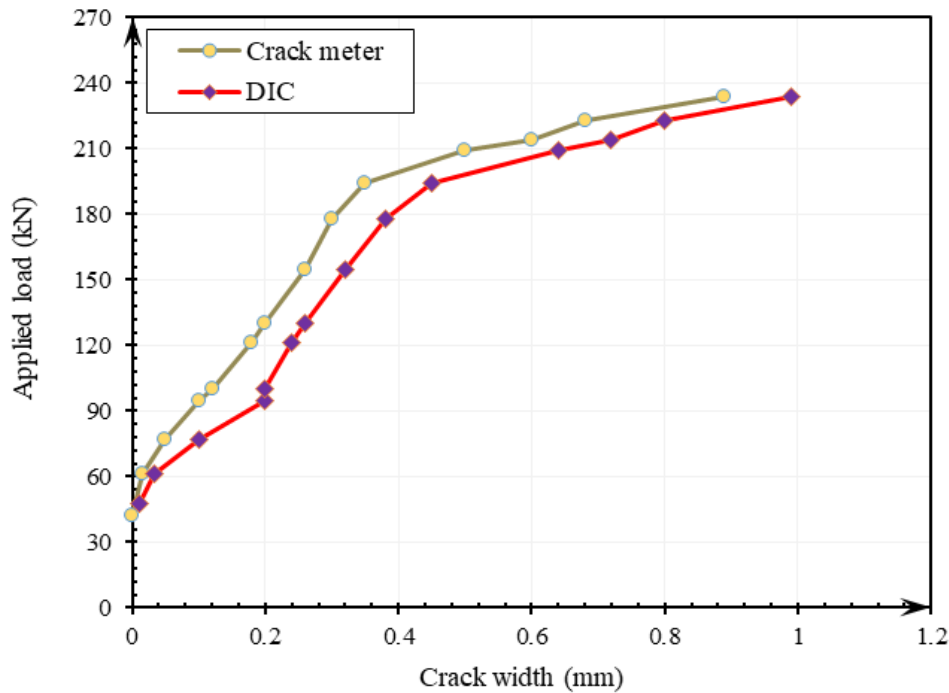


Figure 13. Crack Width Development for Beam F-RA-0.5H.

Declarations

Conflict of Interest

The authors declare that they have no known competing financial interests or personal relationships that could have appeared to influence the work reported in this paper.

Funding

This research did not receive any specific grant from funding agencies in the public, commercial, or not-for-profit sectors.

Declaration on the Use of Generative AI and AI-Assisted Technologies

No generative AI or AI-assisted technologies were used in the preparation of this manuscript.

Data Availability

The data that support the findings of this study are available from the corresponding author upon reasonable request.

Acknowledgement

Great thanks to the staff of the Structural Laboratory at the University of Al-Qadisiyah for their facilities and assistance throughout working on the research..

Ethics

This study did not involve human participants or animals; hence, no ethical approval was required.

References

- Abo Dhaheer, M. S., Al-Rubaye, M. M., Alyhya, W. S., Karihaloo, B. L., & Kulasegaram, S. (2016a). Proportioning of self-compacting concrete mixes based on target plastic viscosity and compressive strength: Part I - mix design procedure. *Journal of Sustainable Cement-Based Materials*, 5(4), 199–216. <https://doi.org/10.1080/21650373.2015.1039625>
- Abo Dhaheer, M. S., Al-Rubaye, M. M., Alyhya, W. S., Karihaloo, B. L., & Kulasegaram, S. (2016b). Proportioning of self-compacting concrete mixes based on target plastic viscosity and compressive strength: Part II - experimental validation. *Journal of Sustainable Cement-Based Materials*, 5(4), 217–232. <https://doi.org/10.1080/21650373.2015.1036952>
- ACI Committee 318. (2019). 318M-19: Building Code Requirements for Structural Concrete and Commentary, Metric. In *Technical Documents* (p. 628). American Concrete Institute. <https://www.concrete.org/publications/internationalconcreteabstractsportal.aspx?m=details&id=51722448>
- Ahmed, W., & Lim, C. W. (2021). Production of sustainable and structural fiber reinforced recycled aggregate concrete with improved fracture properties: A review. *Journal of Cleaner Production*, 279, 123832. <https://doi.org/10.1016/j.jclepro.2020.123832>
- Alam, S. Y., Loukili, A., Grondin, F., & Rozière, E. (2015). Use of the digital image correlation and acoustic emission technique to study the effect of structural size on cracking of reinforced concrete. *Engineering Fracture Mechanics*, 143, 17–31. <https://doi.org/10.1016/j.engfracmech.2015.06.038>

- Alam, S. Y., Saliba, J., & Loukili, A. (2014). Fracture examination in concrete through combined digital image correlation and acoustic emission techniques. *Construction and Building Materials*, 69, 232–242. <https://doi.org/10.1016/j.conbuildmat.2014.07.044>
- Alqarni, A. S., Abbas, H., Al-Shwikh, K. M., & Al-Salloum, Y. A. (2021). Treatment of recycled concrete aggregate to enhance concrete performance. *Construction and Building Materials*, 307, 124960. <https://doi.org/10.1016/j.conbuildmat.2021.124960>
- Al-Rekabi, A. H., & Abo Dhaheer, M. S. (2024). Flexural performance of sustainable hybrid fibre-reinforced SCC beams made of treated recycled aggregates. *Journal of Building Pathology and Rehabilitation*, 9(1), 33. <https://doi.org/10.1007/s41024-023-00382-3>
- Al-Rekabi, A. H., Al-Marmadi, S. M., Dhaheer, M. S. A., & Al-Ramahee, M. (2023). Experimental investigation on sustainable fiber reinforced self-compacting concrete made with treated recycled aggregate. *The Fourth International Conference on Civil and Environmental Engineering Technologies*, 020032. <https://doi.org/10.1063/5.0140655>
- Al-Rekabi, A. H., & Daheer, M. S. A. (2024). Performance of sustainable fiber reinforced concrete with recycled aggregates: A critical review. *The Fourth Al-Noor International Conference for Science and Technology (4NICST2022)*, 060014. <https://doi.org/10.1063/5.0202348>
- André, A., de Brito, J., Rosa, A., & Pedro, D. (2014). Durability performance of concrete incorporating coarse aggregates from marble industry waste. *Journal of Cleaner Production*, 65, 389–396. <https://doi.org/10.1016/j.jclepro.2013.09.037>
- Arezoumandi, M., Smith, A., Volz, J. S., & Khayat, K. H. (2015). An experimental study on flexural strength of reinforced concrete beams with 100% recycled concrete aggregate. *Engineering Structures*, 88, 154–162. <https://doi.org/10.1016/j.engstruct.2015.01.043>
- ASTM International. (2000). *ASTM C1240-01, Specification for Silica Fume Used in Cementitious Mixtures*. ASTM International. <https://doi.org/10.1520/C1240-00E01>
- ASTM International. (2019). *ASTM C494/C494M-24, Specification for Chemical Admixtures for Concrete*. ASTM International. https://doi.org/10.1520/C0494_C0494M-19
- ASTM International. (2022). *ASTM A615/A615M-22, Specification for Deformed and Plain Carbon-Steel Bars for Concrete Reinforcement*. ASTM International. https://doi.org/10.1520/A0615_A0615M-22
- Babu, V. S., Mullick, A. K., Jain, K. K., & Singh, P. K. (2014). Strength and durability characteristics of high-strength concrete with recycled aggregate – influence of mixing techniques. *Journal of Sustainable Cement-Based Materials*, 3(2), 88–110. <https://doi.org/10.1080/21650373.2013.874302>
- Bai, G., Zhu, C., Liu, C., & Liu, B. (2020). An evaluation of the recycled aggregate characteristics and the recycled aggregate concrete mechanical properties. *Construction and Building Materials*, 240, 117978. <https://doi.org/10.1016/j.conbuildmat.2019.117978>
- Bai, W. H., & Sun, B. X. (2010). Experimental Study on Flexural Behavior of Recycled Coarse Aggregate Concrete Beam. *Applied Mechanics and Materials*, 29–32, 543–548. <https://doi.org/10.4028/www.scientific.net/AMM.29-32.543>
- Behnood, A., Olek, J., & Glinicki, M. A. (2015). Predicting modulus elasticity of recycled aggregate concrete using M5' model tree algorithm. *Construction and Building Materials*, 94, 137–147. <https://doi.org/10.1016/j.conbuildmat.2015.06.055>
- Bravo, M., de Brito, J., Pontes, J., & Evangelista, L. (2015). Durability performance of concrete with recycled aggregates from construction and demolition waste plants. *Construction and Building Materials*, 77, 357–369. <https://doi.org/10.1016/j.conbuildmat.2014.12.103>
- Çakır, Ö. (2014). Experimental analysis of properties of recycled coarse aggregate (RCA) concrete with mineral additives. *Construction and Building Materials*, 68, 17–25. <https://doi.org/10.1016/j.conbuildmat.2014.06.032>
- Chen, J. J., Thomas, J. J., & Jennings, H. M. (2006). Decalcification shrinkage of cement paste. *Cement and Concrete Research*, 36(5), 801–809. <https://doi.org/10.1016/j.cemconres.2005.11.003>
- Choi, H., Choi, H., Lim, M., Inoue, M., Kitagaki, R., & Noguchi, T. (2016). Evaluation on the Mechanical Performance of Low-Quality Recycled Aggregate Through Interface Enhancement Between Cement Matrix and Coarse Aggregate by Surface Modification Technology. *International Journal of Concrete Structures and Materials*, 10(1), 87–97. <https://doi.org/10.1007/s40069-015-0124-5>
- Choi, W.-C., Yun, H.-D., & Kim, S.-W. (2012). Flexural performance of reinforced recycled aggregate concrete beams. *Magazine of Concrete Research*, 64(9), 837–848. <https://doi.org/10.1680/macr.11.00018>
- Corinaldesi, V. (2010). Mechanical and elastic behaviour of concretes made of recycled-concrete coarse aggregates. *Construction and Building*

Materials, 24(9), 1616–1620.
<https://doi.org/10.1016/j.conbuildmat.2010.02.031>

Daghash, S. M., & Ozbulut, O. E. (2017). Flexural performance evaluation of NSM basalt FRP-strengthened concrete beams using digital image correlation system. *Composite Structures*, 176, 748–756. <https://doi.org/10.1016/j.compstruct.2017.06.021>

European Guidelines for Self-Compacting Concrete (SCC) | EFCA. (n.d.). <https://www.efca.info/download/european-guidelines-for-self-compacting-concrete-scc/>

Gali, S., & Subramaniam, Kolluru. V. L. (2017). Shear behavior of steel fiber reinforced concrete using full-field displacements from digital image correlation. *MATEC Web of Conferences*, 120, 04003. <https://doi.org/10.1051/mateconf/201712004003>

Gencturk, B., Hossain, K., Kapadia, A., Labib, E., & Mo, Y.-L. (2014). Use of digital image correlation technique in full-scale testing of prestressed concrete structures. *Measurement*, 47, 505–515. <https://doi.org/10.1016/j.measurement.2013.09.018>

Ghahremannejad, M., Mahdavi, M., Saleh, A. E., Abhaee, S., & Abolmaali, A. (2018). Experimental investigation and identification of single and multiple cracks in synthetic fiber concrete beams. *Case Studies in Construction Materials*, 9, e00182. <https://doi.org/10.1016/j.cscm.2018.e00182>

Ghalehnovi, M., Karimipour, A., Anvari, A., & de Brito, J. (2021). Flexural strength enhancement of recycled aggregate concrete beams with steel fibre-reinforced concrete jacket. *Engineering Structures*, 240, 112325. <https://doi.org/10.1016/j.engstruct.2021.112325>

Ghoneim, M., Yehia, A., Yehia, S., & Abuzaid, W. (2020). Shear Strength of Fiber Reinforced Recycled Aggregate Concrete. *Materials*, 13(18), 4183. <https://doi.org/10.3390/ma13184183>

Grdić, D. Z., Topličić-Ćurčić, G. A., Grdić, Z. J., & Ristić, N. S. (2021). Durability Properties of Concrete Supplemented with Recycled CRT Glass as Cementitious Material. *Materials*, 14(16), 4421. <https://doi.org/10.3390/ma14164421>

Hamad, B. S., & Dawi, A. H. (2017). Sustainable normal and high strength recycled aggregate concretes using crushed tested cylinders as coarse aggregates. *Case Studies in Construction Materials*, 7, 228–239. <https://doi.org/10.1016/j.cscm.2017.08.006>

Ignjatović, I. S., Marinković, S. B., Mišković, Z. M., & Savić, A. R. (2013). Flexural behavior of reinforced recycled aggregate concrete beams under short-term loading. *Materials and Structures*, 46(6),

1045–1059. <https://doi.org/10.1617/s11527-012-9952-9>

IQS 5. (1984). *Iraqi Standard Specification No.5, for Portland cement Central Organization for Standardization and Quality.*

IQS 45. (1984). *Iraqi Standard Specification No.5, for Aggregate Central Organization for Standardization and Quality.*

Jiang, C., Fan, K., Wu, F., & Chen, D. (2014). Experimental study on the mechanical properties and microstructure of chopped basalt fibre reinforced concrete. *Materials & Design*, 58, 187–193. <https://doi.org/10.1016/j.matdes.2014.01.056>

Kannam, P., Kannam, P., Sarella, V. R., & Pancharathi, R. K. (2018). Influence of Recycled Aggregate on Shear Behavior of Steel Fibrous SCC. *Journal of Materials and Engineering Structures «JMES»*, 5(2), 185–205. <https://revue.ummto.dz/index.php/JMES/article/view/1714>

Knaack, A. M., & Kurama, Y. C. (2015). Behavior of Reinforced Concrete Beams with Recycled Concrete Coarse Aggregates. *Journal of Structural Engineering*, 141(3). [https://doi.org/10.1061/\(ASCE\)ST.1943-541X.0001118](https://doi.org/10.1061/(ASCE)ST.1943-541X.0001118)

Kou, S. C., & Poon, C. S. (2009). Properties of self-compacting concrete prepared with coarse and fine recycled concrete aggregates. *Cement and Concrete Composites*, 31(9), 622–627. <https://doi.org/10.1016/j.cemconcomp.2009.06.005>

Kou, S.-C., Poon, C.-S., & Wan, H.-W. (2012). Properties of concrete prepared with low-grade recycled aggregates. *Construction and Building Materials*, 36, 881–889. <https://doi.org/10.1016/j.conbuildmat.2012.06.060>

Mohammed Abd, L. (2018). Behavior Of Reinforced Self-Compacting Concrete Beams Containing Steel Fibers And Recycled Coarse Aggregates. *Journal of Engineering and Sustainable Development*, 2018(05), 170–187. <https://doi.org/10.31272/jeasd.2018.5.13>

Muhsin Farhood, A., Abdul, J., & Khudhair, S. (2018). Shear Strength of Self Compacting Concrete made with Recycled Concrete as Coarse Aggregate. *University of Thi-Qar Journal*, 13(2), 119–137. <https://jutq.utq.edu.iq/index.php/main/article/view/144>

Mukai, T., & Kikuchi, M. (2023). Properties of Reinforced Concrete Beams Containing Recycled Aggregate. In *Demolition Reuse Conc Mason V2* (1st ed., pp. 670–679). CRC Press. <https://doi.org/10.1201/9781003416562-20>

- Panda, K. C., & Bal, P. K. (2013). Properties of Self Compacting Concrete Using Recycled Coarse Aggregate. *Procedia Engineering*, 51, 159–164. <https://doi.org/10.1016/j.proeng.2013.01.023>
- Pedro, D., de Brito, J., & Evangelista, L. (2015). Performance of concrete made with aggregates recycled from precasting industry waste: influence of the crushing process. *Materials and Structures*, 48(12), 3965–3978. <https://doi.org/10.1617/s11527-014-0456-7>
- Peters, W. H., Ranson, W. F., Sutton, M. A., Chu, T. C., & Anderson, J. (1983). Application Of Digital Correlation Methods to Rigid Body Mechanics. *Optical Engineering*, 22(6). <https://doi.org/10.1117/12.7973231>
- Pradhan, S., Kumar, S., & Barai, S. V. (2018). Performance of reinforced recycled aggregate concrete beams in flexure: experimental and critical comparative analysis. *Materials and Structures*, 51(3), 58. <https://doi.org/10.1617/s11527-018-1185-0>
- Ruocci, G., Rospars, C., Moreau, G., Bisch, P., Erlicher, S., Delaplace, A., & Henault, J. -M. (2016). Digital Image Correlation and Noise-filtering Approach for the Cracking Assessment of Massive Reinforced Concrete Structures. *Strain*, 52(6), 503–521. <https://doi.org/10.1111/str.12192>
- Sayhood, E., Resheq, A., & Raof, F. (2019). Behavior of Recycled Aggregate Fibrous Reinforced Beams Under Flexural and Shear Loading. *Engineering and Technology Journal*, 37(3C), 338–344. <https://doi.org/10.30684/etj.37.3C.6>
- Seara-Paz, S., González-Fontebao, B., Martínez-Abella, F., & Eiras-López, J. (2018). Flexural performance of reinforced concrete beams made with recycled concrete coarse aggregate. *Engineering Structures*, 156, 32–45. <https://doi.org/10.1016/j.engstruct.2017.11.015>
- Seo, D. S., & Choi, H. B. (2014). Effects of the old cement mortar attached to the recycled aggregate surface on the bond characteristics between aggregate and cement mortar. *Construction and Building Materials*, 59, 72–77. <https://doi.org/10.1016/j.conbuildmat.2014.02.047>
- Shi, C., Li, Y., Zhang, J., Li, W., Chong, L., & Xie, Z. (2016). Performance enhancement of recycled concrete aggregate – A review. *Journal of Cleaner Production*, 112, 466–472. <https://doi.org/10.1016/j.jclepro.2015.08.057>
- Singh, A., Duan, Z., Xiao, J., & Liu, Q. (2020). Incorporating recycled aggregates in self-compacting concrete: a review. *Journal of Sustainable Cement-Based Materials*, 9(3), 165–189. <https://doi.org/10.1080/21650373.2019.1706205>
- State of the aggregate resource in Ontario study: consolidated report. (2010). Ontario Ministry of Natural Resources.
- Suryanto, B., Tambusay, A., & Suprobo, P. (2017). Crack Mapping on Shear-critical Reinforced Concrete Beams using an Open Source Digital Image Correlation Software. *Civil Engineering Dimension*, 19(2). <https://doi.org/10.9744/ced.19.2.93-98>
- Tam, V. W. Y., Soomro, M., & Evangelista, A. C. J. (2018). A review of recycled aggregate in concrete applications (2000–2017). *Construction and Building Materials*, 172, 272–292. <https://doi.org/10.1016/j.conbuildmat.2018.03.240>
- Tam, V. W. Y., & Tam, C. M. (2008). Diversifying two-stage mixing approach (TSMA) for recycled aggregate concrete: TSMA and TSMA_{sc}. *Construction and Building Materials*, 22(10), 2068–2077. <https://doi.org/10.1016/j.conbuildmat.2007.07.024>
- Tam, V. W. Y., Tam, C. M., & Wang, Y. (2007). Optimization on proportion for recycled aggregate in concrete using two-stage mixing approach. *Construction and Building Materials*, 21(10), 1928–1939. <https://doi.org/10.1016/j.conbuildmat.2006.05.040>
- Tam, V. W.-Y., Gao, X.-F., & Tam, C. M. (2006). Comparing performance of modified two-stage mixing approach for producing recycled aggregate concrete. *Magazine of Concrete Research*, 58(7), 477–484. <https://doi.org/10.1680/mac.2006.58.7.477>
- Visintin, P., Xie, T., & Bennett, B. (2020). A large-scale life-cycle assessment of recycled aggregate concrete: The influence of functional unit, emissions allocation and carbon dioxide uptake. *Journal of Cleaner Production*, 248, 119243. <https://doi.org/10.1016/j.jclepro.2019.119243>
- Wang, Y., Hughes, P., Niu, H., & Fan, Y. (2019). A new method to improve the properties of recycled aggregate concrete: Composite addition of basalt fiber and nano-silica. *Journal of Cleaner Production*, 236, 117602. <https://doi.org/10.1016/j.jclepro.2019.07.077>
- Xia, D., Xie, S., Fu, M., & Zhu, F. (2021). Effects of maximum particle size of coarse aggregates and steel fiber contents on the mechanical properties and impact resistance of recycled aggregate concrete. *Advances in Structural Engineering*, 24(13), 3085–3098. <https://doi.org/10.1177/13694332211017998>
- Xie, J., Kou, S., Ma, H., Long, W.-J., Wang, Y., & Ye, T.-H. (2021). Advances on properties of fiber reinforced recycled aggregate concrete: Experiments and models. *Construction and Building Materials*, 277, 122345. <https://doi.org/10.1016/j.conbuildmat.2021.122345>

Yang, S., & Lee, H. (2017). Structural Performance of Reinforced RCA Concrete Beams Made by a Modified EMV Method. *Sustainability*, 9(1), 131. <https://doi.org/10.3390/su9010131>

Yehia, S., AlHamaydeh, M., & Farrag, S. (2014). High-Strength Lightweight SCC Matrix with Partial Normal-Weight Coarse-Aggregate Replacement: Strength and Durability Evaluations. *Journal of Materials in Civil Engineering*, 26(11). [https://doi.org/10.1061/\(ASCE\)MT.1943-5533.0000990](https://doi.org/10.1061/(ASCE)MT.1943-5533.0000990)

Yehia, S., Farrag, S., Abu-Sharhk, A., Zaher, A., Istayteh, H., & Helal, K. (2015, April 13). Concrete with Recycled Aggregate: Evaluation of Mechanical Properties. *3rd Annual International Conference on Architecture and Civil Engineering (ACE 2015)*. https://doi.org/10.5176/2301-394X_ACE15.65

Yehia, S., Helal, K., Abusharkh, A., Zaher, A., & Istaitiyeh, H. (2015). Strength and Durability Evaluation of Recycled Aggregate Concrete. *International Journal of Concrete Structures and Materials*, 9(2), 219–239. <https://doi.org/10.1007/s40069-015-0100-0>

Yildirim, S. T., Meyer, C., & Herfellner, S. (2015). Effects of internal curing on the strength, drying shrinkage and freeze–thaw resistance of concrete containing recycled concrete aggregates. *Construction and Building Materials*, 91, 288–296. <https://doi.org/10.1016/j.conbuildmat.2015.05.045>